

New structures and properties of YF_3 and YF_6 under high pressure

Lebin Chang(常乐斌), Jianlun Huang(黄健伦), Yuhao Fu(付钰豪), Yingying Wang(王莹莹), and Jurong Zhang(张车荣)

Citation: Chin. Phys. B, 2026, 35 (**3**): 036301. DOI: 10.1088/1674-1056/ae1f02
http://cpb.iphy.ac.cn; http://iopscience.iop.org/cpb

What follows is a list of articles you may be interested in

Anomalous lattice vibration in monolayer MoS_2 induced by DUV laser: A first-principles investigation

Weidong Wang(王卫东), Renhui Liu(刘仁辉), Ye Zhang(张也), Huaihong Guo(郭怀红), Jianqi Huang(黄建啟), Zhantong Liu(刘展彤), Heting Zhao(赵贺霆), Kai Wang(王凯), Bo Zhao(赵波), and Teng Yang(杨腾)
Chin. Phys. B, 2025, 34 (**6**): 066301. DOI: 10.1088/1674-1056/adc36e

Unveiling phonon frequency-dependent mechanism of heat transport across stacking fault in silicon carbide

Fu Wang(王甫), Yandong Sun(孙彦东), Yu Zou(邹宇), Ben Xu(徐贲), and Baoqin Fu(付宝勤)
Chin. Phys. B, 2023, 32 (**9**): 096301. DOI: 10.1088/1674-1056/acdfc0

Inverted V-shaped evolution of superconducting temperature in SrBC under pressure

Ru-Yi Zhao(赵如意), Xun-Wang Yan(闫循旺), and Miao Gao(高淼)
Chin. Phys. B, 2021, 30 (**7**): 076301. DOI: 10.1088/1674-1056/abfbcc

Raman scattering study of two-dimensional magnetic van der Waals compound VI_3

Yi-Meng Wang(王艺朦), Shang-Jie Tian(田尚杰), Cheng-He Li(李承贺), Feng Jin(金峰), Jian-Ting Ji(籍建葶), He-Chang Lei(雷和畅), Qing-Ming Zhang(张清明)
Chin. Phys. B, 2020, 29 (**5**): 056301. DOI: 10.1088/1674-1056/ab8215

Raman scattering study of magnetic layered MPS_3 crystals (M=Mn, Fe, Ni)

Yi-Meng Wang(王艺朦), Jian-Feng Zhang(张建丰), Cheng-He Li(李承贺), Xiao-Li Ma(马肖莉), Jian-Ting Ji(籍建葶), Feng Jin(金峰), He-Chang Lei(雷和畅), Kai Liu(刘凯), Wei-Lu Zhang(张玮璐), Qing-Ming Zhang(张清明)
Chin. Phys. B, 2019, 28 (**5**): 056301. DOI: 10.1088/1674-1056/28/5/056301

SPECIAL TOPIC — Structures and properties of materials under high pressure

New structures and properties of YF_3 and YF_6 under high pressure

Lebin Chang(常乐斌)[1], Jianlun Huang(黄健伦)[1], Yuhao Fu(付钰豪)[2], Yingying Wang(王莹莹)[3,†], and Jurong Zhang(张车荣)[1,‡]

[1] *School of Physics and Electronics, Shandong Normal University, Jinan* 250014, *China*
[2] *College of Physics, Jilin University, Changchun* 130012, *China*
[3] *School of Physics and Electronic Engineering, Qilu Normal University, Jinan* 250200, *China*

(Received 28 September 2025; revised manuscript received 10 November 2025; accepted manuscript online 13 November 2025)

Exploring new structures and properties of matter is a central topic in condensed matter physics. In this work, first-principles calculations and structure prediction methods were employed to investigate fluorine-rich yttrium compounds. Two new stable phases, *Pmmn*-YF_3 and *Amm*2-YF_6, have been identified under high pressure. *Pmmn*-YF_3 is stable over a pressure range of 50 GPa to 500 GPa, and *Amm*2-YF_6 remains stable at pressures beyond 429 GPa. Analysis of the band structure, density of states (DOS), and Bader charge for these two stable compounds reveals that *Pmmn*-YF_3 is an insulator and *Amm*2-YF_6 is a metal, elucidating their chemical bonding characteristics. F–F bond lengths and Bader charge analysis confirm the +3 oxidation state of yttrium in the molecular crystal YF_3 and the crystal structure YF_6. Our work provides a valuable theoretical foundation for elucidating the properties of the rare earth transition metal yttrium.

Keywords: lattice dynamics, first-principles theory, solid–solid transitions, crystallographic aspects of phase transformations, pressure effects

PACS: 63.20.dk, 61.50.Ks

DOI: 10.1088/1674-1056/ae1f02 **CSTR:** 32038.14.CPB.ae1f02

1. Introduction

Yttrium, a rare earth metal, has been the subject of extensive investigations into its stable space group, crystal structure, and electronic properties under ultrahigh pressure.[1–3] The valence electrons of yttrium primarily reside in the outermost 5s orbital and the second outermost 4d orbital. The 5s orbital is fully occupied with two electrons, and the 4d orbital is occupied by one electron.[4] This configuration determines the chemical properties of yttrium. It readily loses its three valence electrons to form a trivalent cation, which is the most common oxidation state of yttrium.[4,5] The electronegativity value of yttrium is 1.22.[6] The compounds of yttrium (Y) exhibit unique physical and chemical properties, leading to extensive applications in various fields. Yttrium barium copper oxide ($YBa_2Cu_3O_{7-x}$, YBCO)[7,8] is one of the most representative high-temperature superconducting materials. It exhibits a critical temperature of approximately 90 K.[8] This material is used to manufacture superconducting cables, superconducting magnets, and superconducting motors,[9] with efficiency far exceeding that of conventional conductors. Owing to the clathrate structures of yttrium superhydrides (YH_6,[10–13] YH_9[11–14]), they have high superconducting critical temperatures, making them promising candidates for room-temperature superconductors.[15,16] Yttrium oxide has a high dielectric constant and thermal stability, which makes it useful as a polarizer.[17] Therefore, exploring yttrium and its compounds to discover new physical and chemical properties could lead to important practical applications.

Fluorine has seven electrons in its outermost shell, making it highly prone to gaining one electron to form the stable fluoride ion (F^-). Its electronegativity is 3.98,[6] which is the highest among known elements and one of the strongest oxidizing agents. Fluorine, as an oxidizing agent, can undergo intense reactions with other elements, obtaining electrons from them to change their valence states, thereby forming new physical and chemical properties.[18] The only fluoride of yttrium that has been discovered so far is yttrium trifluoride (YF_3), and its crystal structure is orthorhombic with the *Pnma* space group.[19–21] Yttrium fluoride has a high refractive index and transparency, and can be used for coating optical lenses and as a material for crystal lasers.[22] The band gap of YF_3 is 7.58 eV according to density functional calculations and is estimated to be 12.5 eV from spectral emissions. Therefore, it is necessary to study other structures of YF_3, as well as other stoichiometries and their physical and chemical properties in this system.

High pressure can alter the physical and chemical properties of elements at normal pressure, creating new chemical structures, unconventional stoichiometry, and extraordinary physical and chemical properties.[23–26] Recent studies

†Corresponding author. E-mail: yywang@qlnu.edu.cn
‡Corresponding author. E-mail: zjr@calypso.cn

© 2026 Chinese Physical Society and IOP Publishing Ltd. All rights, including for text and data mining, AI training, and similar technologies, are reserved.

of unknown high oxidation states, such as Au^{4+} in AuF_4 and Au^{6+} in AuF_6,[24] as well as Hg^{3+} and Hg^{4+} in HgF_3 and HgF_4,[25,26] and the exotic helium-bearing compounds (FeOOHe[27] and FeF_3He[28]) that do not exist at normal pressure, demonstrate that unconventional stoichiometry emerges under high pressure. For example, NH_{10}, NH_{11}, and NH_{12} are stabilized by NH_4 units,[29] and the transition of metals to semiconductors at high pressure highlights the significance and necessity of high-pressure technology in uncovering new properties.

In this study, a systematic investigation of the Y–F system under high pressure was performed using a combination of first-principles calculations and structural prediction methods. It was confirmed that YF_3 exists stably under ambient pressure, and new high-pressure phases of YF_3 were discovered. Additionally, a novel stoichiometric phase YF_6 was found to be stable at 429 GPa. Interestingly, electronic property calculations show that both the ambient pressure and high-pressure phases of YF_3 are insulators, while YF_6 is a metal. The thermodynamic and kinetic stability of these new phases, as well as their diffusion properties at 300 K, have all been calculated. These results deepen our understanding of the properties of yttrium fluoride compounds.

2. Computation detail

The CALYPSO prediction method and code[30,31] were used to search for stable structures in the Y–F system at ultrahigh pressures of 100 GPa, 300 GPa, and 500 GPa. The search targeted stoichiometries with 1–4 formula units per cell, constrained to a maximum of 36 atoms. Our calculations were based on the principles of density functional theory (DFT).[32] The Perdew–Burke–Ernzerhof (PBE) exchange-correlation functional,[33] generalized gradient approximation (GGA),[34] and all-electron projector-augmented wave potentials in the Vienna *ab initio* simulation package (VASP)[35] code were used in the calculations. We set the cutoff energy at 800 eV and used a Monkhorst–Pack *k*-point grid sampled at a spacing of $2\pi \times 0.03$ Å^{-1} in the Brillouin zone. The valence electrons considered for F and Y atoms were $2s^2 2p^5$ and $4s^2 4p^6 4d^1 5s^2$, respectively. The Phonopy[36] code was used to calculate the phonon spectrum via the finite displacement method. The interaction between yttrium and fluorine was analyzed using the crystal orbital Hamilton population (COHP).[37] *Ab initio* molecular dynamics (AIMD) simulations were performed in the canonical (NVT) ensemble using a Nosé thermostat.[38] The simulations spanned 20 ps, with the initial 2–5 ps allocated to system equilibration. The simulation cells for YF_3 and YF_6 contained 144 and 189 atoms, respectively.

3. Result and discussion

In this study, an intelligent structure search was performed on fluorine-rich YF_n (n = 1–8) systems with the objective of identifying thermodynamically stable compositions at corresponding pressures. By calculating the formation enthalpies relative to the dissociation products of the constituent elements and using the formula

$$\Delta H = \frac{H(\mathrm{YF}_n) - H(\mathrm{Y}) - nH(\mathrm{F})}{n+1},$$

convex hull diagrams of the Y–F system at various pressures were constructed, as shown in Figs. 1(a) and 1(b). In the pressure range of 300–500 GPa, the *Cmca* phase is stable for fluorine,[39–41] and the *Fddd* phase is stable for yttrium.[1] Y–F compounds positioned on the convex hull are thermodynamically stable, characterized by a lower decomposition tendency

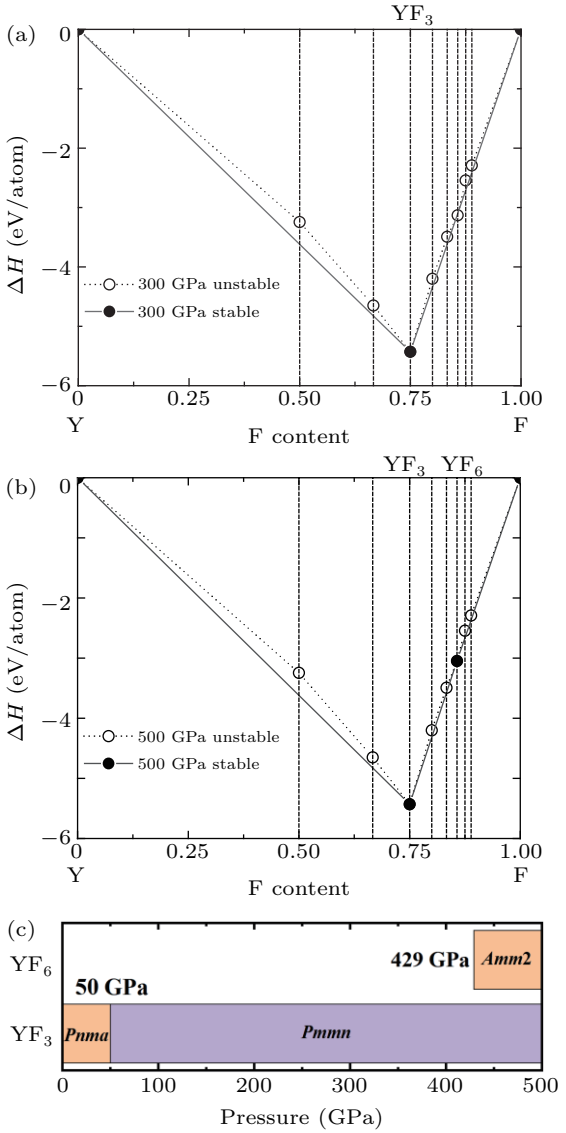


Fig. 1. (a) Convex hull of YF_n (n = 1–8) compounds under 300 GPa. (b) Convex hull of Y–F compounds under 500 GPa. Compounds located on the solid line (filled symbols) are thermodynamically stable; compounds positioned on the dotted line (unfilled symbols) are metastable. (c) Pressure-composition phase diagram of the Y–F system in the range 0–500 GPa.

and potential synthetic feasibility. In contrast, phases positioned above the convex hull are thermodynamically unstable. Figure 1(a) shows that YF_3 is thermodynamically stable at 300 GPa, and Fig. 1(b) indicates that both YF_3 and YF_6 are thermodynamically stable at 500 GPa. To confirm the stable pressure ranges of YF_3 and YF_6, we calculated a pressure-composition phase diagram, as shown in Fig. 1(c). It illustrates that *Pnma*-YF_3 is stable between 0 GPa and 50 GPa, *Pmmn*-YF_3 becomes stable above 50 GPa, and *Amm*2-YF_6 exhibits stability above 429 GPa. The *Pnma*-YF_3 stable structure we calculated is consistent with the one previously reported[19–21] at atmospheric pressure, which verifies the reliability of our calculation results.

Phonon dispersion calculations were conducted for these phases to evaluate their dynamic stability, with results presented in Fig. 2. No imaginary frequencies are observed in the calculated phonon spectra throughout the entire Brillouin zone, confirming the dynamic stability of *Pmmn*-YF_3 and *Amm*2-YF_6 under their respective pressures. Thus, it can be concluded that the *Pmmn*-YF_3 and *Amm*2-YF_6 structures are both thermodynamically and kinetically stable under their respective pressures.

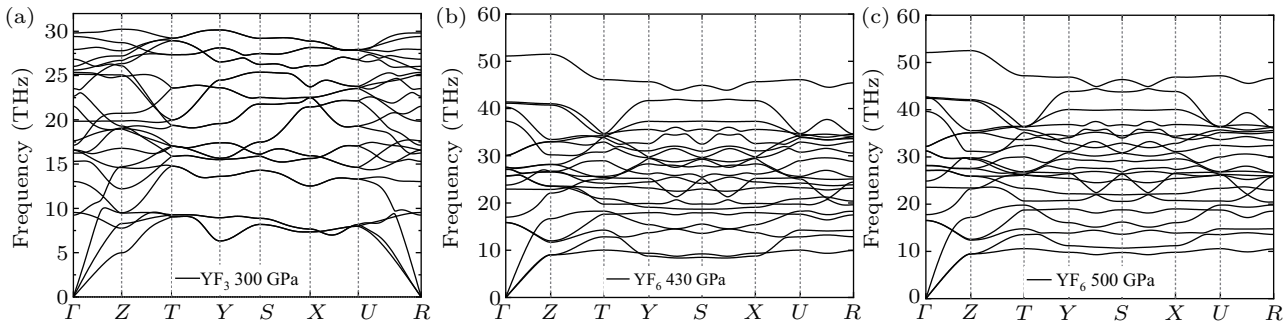


Fig. 2. Phonon dispersion curves for (a) *Pmmn*-YF_3 at 300 GPa, (b) *Amm*2-YF_6 at 430 GPa, and (c) *Amm*2-YF_6 at 500 GPa.

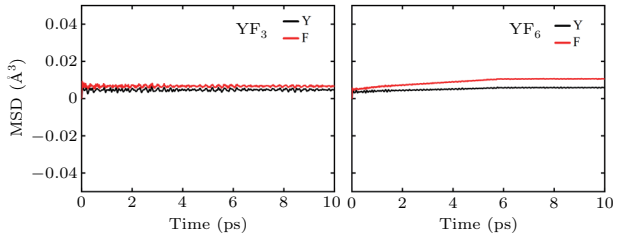


Fig. 3. Mean-square displacement (MSD) of yttrium and fluorine in (a) YF_3 at a density of 10.02 g/cm^3, and (b) YF_6 at a density of 11.21 g/cm^3 at 300 K.

AIMD simulations were performed to quantitatively characterize the extent of atomic displacement. Figure 3 shows the simulated mean-square displacement (MSD) of YF_3 at a density of 10.02 g/cm^3 and YF_6 at a density of 11.20 g/cm^3. For both YF_3 and YF_6, the MSD values of the Y and F atoms remain nearly constant, indicating that the system is stable in the solid state, with all atoms vibrating around their equilibrium positions.

The crystal structures of *Pnma*-YF_3, *Pmmn*-YF_3, and *Amm*2-YF_6 are shown in Fig. 4, while the lattice parameters and atomic coordinates for *Pmmn*-YF_3 at 300 GPa and *Amm*2-YF_6 at 500 GPa are tabulated in Table 1. For *Pnma*-YF_3 at ambient pressure, each Y atom coordinates with eight F atoms, located at the center of an F_8 cage. In *Pnma*-YF_3, the lengths of the nearest Y–F and F–F bonds are 2.20 Å and 2.58 Å, respectively. The F–F bond length is much longer than the 1.44 Å of a covalent F–F bond.[24]

For *Pmmn*-YF_3 at 300 GPa, F atoms form an F_{12} cage, with Y atoms residing at the center; each Y atom coordinates with twelve F atoms. Analogous to the cage-like structure formed by H atoms in *I*4/*mmm*-YH_3, H atoms in YH_3 form an H_{14} cage.[42] For *Pmmn*-YF_3, the nearest Y–F bond length is 2.02 Å, and the shortest F–F bond length is 2.03 Å, much longer than 1.44 Å[24] of a covalent F–F bond. The phase transition from *Pnma*-YF_3 to *Pmmn*-YF_3 at 50 GPa is characterized by a reduction in Y–F and F–F bond lengths, an increase in the Y coordination number, and a change in the F cage from F_8 to F_{12}.

For *Amm*2-YF_6 at 500 GPa, the structure exhibits relatively high symmetry. Compared to *Pmmn*-YF_3, the F atoms in YF_6 form an F_{15} cage, with Y atoms positioned at the center and exhibiting a higher coordination number. Analogous to the cage-like structure formed by H atoms in *Im*-3*m*-YH_6, the H atoms in YH_6 form an H_{24} cage.[42] For *Amm*2-YF_6, the nearest Y–F and F–F distances are 1.91 Å and 1.64 Å, respectively. The F–F distance is longer than that of a covalent F–F bond (1.44 Å[24]), indicating that the F–F bonds in YF_6 are not covalent.

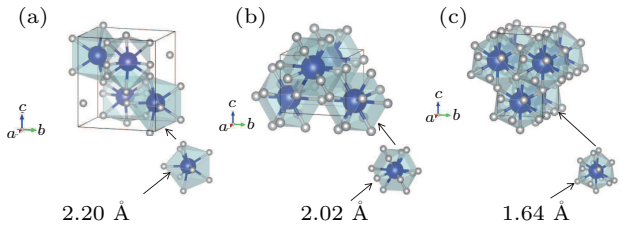


Fig. 4. Crystal structures of (a) *Pnma*-YF_3 at 0 GPa, (b) *Pmmn*-YF_3 at 300 GPa, and (c) *Amm*2-YF_6 at 500 GPa. In this depiction, blue and gray spheres represent Y and F atoms, respectively.

For a more in-depth understanding of the electronic structure and bonding characteristics of yttrium-fluorine compounds, the electron localization function (ELF) was computed, and the results are presented in Fig. 5. It is well established that ELF values greater than 0.5 are associated with lone pairs, core electrons, or covalent bonds, with an ELF value of 1 indicating complete electron localization. Ionic bonding, by contrast, is associated with lower ELF values (< 0.5), where ELF $= 0$ corresponds to complete electron delocalization. For metallic bonding, the typical ELF value is 0.5, indicating an electron pairing distribution analogous to that of a free electron gas.[43]

For *Pmmn*-YF_3, the highest ELF values are localized near F atoms, approaching 0.82, indicating strong electron localization in the vicinity of F atoms. ELF values in the Y–F and F–F interatomic regions are approximately 0.18 and 0.09, respectively, indicating that Y–F bonds are dominated by ionic character and that no covalent bonds are formed between F atoms. Similar to HgF_3, the regions surrounding F atoms in our system also exhibit extremely low ELF values,[25] suggesting a lack of significant covalent bonding character between these F atoms and other atoms.

The ELF characteristics of *Amm*2-YF_6 are analogous to those of YF_3. High values of approximately 0.82 are localized near F atoms, while values in the Y–F and F–F interatomic regions are very low, approaching 0.13 and 0.08, respectively. These low values confirm that the bonding in YF_6 is primarily ionic.

Table 1. Structural parameters of *Pmmn*-YF_3 at 300 GPa and *Amm*2-YF_6 at 500 GPa.

Space group parameters	Lattice (Å)		Atom coordinates (fractional)			
Pmmn-YF_3	$a = 3.344$, $b = 4.161$, $c = 3.476$	Y1	0.500	0.00	0.188	1*a*
	$\alpha = \beta = \gamma = 90°$	Y2	0.00	0.500	0.812	1*a*
		F1	0.500	0.250	0.679	1*a*
		F2	0.00	0.250	0.321	1*a*
		F3	0.00	0.00	0.825	1*a*
		F4	0.00	0.750	0.321	1*a*
		F5	0.500	0.750	0.679	1*a*
		F6	0.500	0.500	0.175	1*a*
*Amm*2-YF_6	$a = 3.320$, $b = 3.232$, $c = 5.599$	Y1	0.00	−0.500	0.167	2*a*
	$\alpha = \beta = \gamma = 90°$	F1	−0.240	−0.500	0.500	2*a*
		F2	−0.00	−0.500	−0.167	4*c*
		F3	−0.500	−0.745	−0.248	4*e*
		F4	−0.500	−0.500	−0.003	2*b*

Table 2. Bader charges of *Pmmn*-YF_3 and *Amm*2-YF_6.

Compound	Pressure (GPa)	Δ*e*/atom (Y)	Δ*e*/atom (F)
Pmmn-YF_3	300	2.20 *e*	−0.74 *e*/ − 0.73 *e*
	500	2.21 *e*	−0.74 *e*/ − 0.73 *e*
*Amm*2-YF_6	300	2.25 *e*	-0.70 *e*/ − 0.40 *e*/ − 0.25 *e*
	500	2.20 *e*	−0.70 *e*/ − 0.39 *e*/ − 0.24 *e*

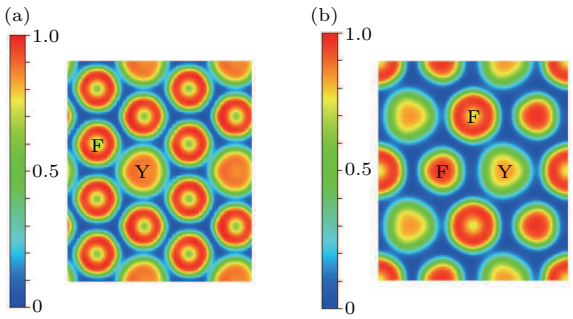


Fig. 5. Electron Localization Function (ELF) maps for (a) *Pmmn*-YF_3 on the (100) plane at 300 GPa, and (b) *Amm*2-YF_6 on the (100) plane at 500 GPa.

Bader charge analysis was conducted on YF_3 and YF_6 to quantify the electron transfer between yttrium and fluorine atoms (Table 2). In Y–F systems, yttrium atoms function as electron donors, whereas fluorine atoms act as electron acceptors. For *Pmmn*-YF_3 at 300 GPa, each Y atom donates 2.20 electrons to the surrounding F atoms. According to the bonding type and Bader charge, fluorine atoms fall into two distinct types: one type, with only one fluorine atom, gains 0.74 electrons; the other type, with two fluorine atoms, gains 0.73 electrons.

For *Amm*2-YF_6 at 500 GPa, each Y atom donates 2.20 electrons. F atoms fall into three distinct types: the first type, with two fluorine atoms, gains 0.39 electrons; the second type, with three fluorine atoms, gains 0.24 electrons; the third type gains 0.70 electrons.

Previous studies have established that Y_2O_3 is stable under ambient conditions due to the Gibbs–Thomson effect, and that yttrium exhibits a +3 valence state in this compound.[44] Previous calculations on yttrium oxides with exotic stoichiometries showed that the Bader charges of Y1 and Y2 in YO_3 at 100 GPa are 2.04 and 2.12 electrons, respectively. These values are close to the 2.12 electrons calculated for *Ia*-3-Y_2O_3 at 1 atm, indicating that Y in YO_3 is in the +3 oxidation state.[4] Subsequently, the high-pressure phase transition of yttrium monoxide was discovered: upon compression, *Fm*-3*m*-YO transforms into *Pm*-3*m*-YO. The absolute Bader charge value of Y in both *Fm*-3*m*-YO and *Pm*-3*m*-YO is close to that of O in their respective structures, indicating that Y has

a +2 formal oxidation state in YO.[4]

Research on nitrogen-rich yttrium compounds has identified the stable phase $P2_1$-YN_2 at ambient pressure.[45] It is composed of Y^{2+} cations and N_2^{2-} anions, and the valence state of Y in YN_2 is +2.[45] In studies on the reaction between Y^+ and molecular oxygen or carbon monoxide, Y^+ was observed mostly in its ground state using a flow tube (FT) ion source, confirming the existence of Y^+.[46] Through theoretical research on the first and second rows of transition metals, and by comparing Y^+ with Sc^+, it was found that Y^+ has a $5s^2$ (^{1}S) ground state, which has lower energy than other states ($4d^15s^1$ (^{3}D), $4d^15s^1$ (^{1}D), $4d^2$ (^{3}F)).[47]

The F–F bond length in YF_3 is calculated to be 2.03 Å, much longer than the covalent F–F bond length of 1.44 Å, which indicates that *Pmmn*-YF_3 is a molecular crystal. Given that Y loses 2.20 electrons in the *Pmmn* phase and the molecular crystal characteristics of YF_3, Y in YF_3 is in the +3 oxidation state. The calculated Bader charge for Y in *Amm*2-YF_6 at 500 GPa is 2.20 electrons, identical to the value in *Pmmn*-YF_3 at 300 GPa and close to the 2.12 electrons in *Ia*-3-Y_2O_3 at 1 atm, indicating that the oxidation state of Y in YF_6 is also +3.

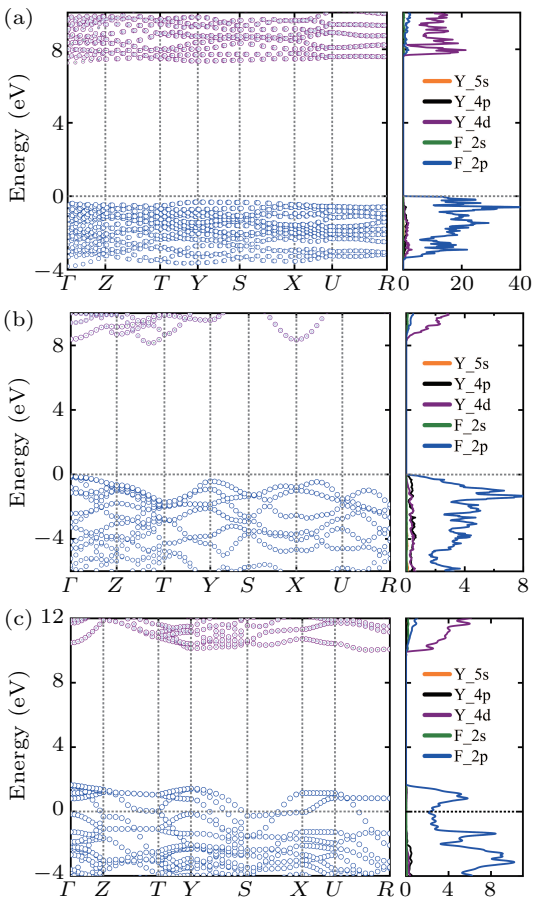


Fig. 6. Electronic band structure and projected density of states (PDOS) of (a) *Pnma*-YF_3 at 0 GPa, (b) *Pmmn*-YF_3 at 300 GPa, and (c) *Amm*2-YF_6 at 500 GPa. The Fermi energy (black dashed line) is set to zero.

The band structure and projected density of states (PDOS) for *Pnma*-YF_3, *Pmmn*-YF_3, and *Amm*2-YF_6 are presented in Fig. 6. The new *Pmmn* phase of YF_3 is an indirect bandgap insulator with a band gap of approximately 8.14 eV. At ambient pressure, the *Pnma* phase of YF_3 is also an insulator with a band gap of ∼ 7.58 eV, similar to that of the *Pmmn* phase.

As observed from the DOS diagrams, below the Fermi level, F-2p orbitals are predominant, whereas above the Fermi level, Y-4d orbitals dominate. At the Fermi level, *Amm*2-YF_6 shows an overlap between the conduction and valence bands, classifying it as a metal. The overlap of conduction and valence bands under high pressure signifies metallic behavior in *R*-3-AuF_6,[24] *C*2/*c*-OsF_6,[48] and *Pnma*-IrF_6.[49] Unlike YF_6, the d orbitals of the metal are primarily dominant at the Fermi level. The band structure of *Amm*2-YF_6 is relatively flat, implying a high effective mass and hence low carrier mobility.[50]

Figure 6(b) shows that F-2p orbitals dominate at the Fermi level, while contributions from F-2s, Y-4d, and Y-4p orbitals are minor but nearly equal, as seen in the rightmost panel. Similar to *Cmcm*-YO_3 and *Fm*-3*m*-YO, at the Fermi level, the O-2p orbitals dominate, with minor but nearly equal contributions from O-2s, Y-4d, and Y-4p orbitals.[4]

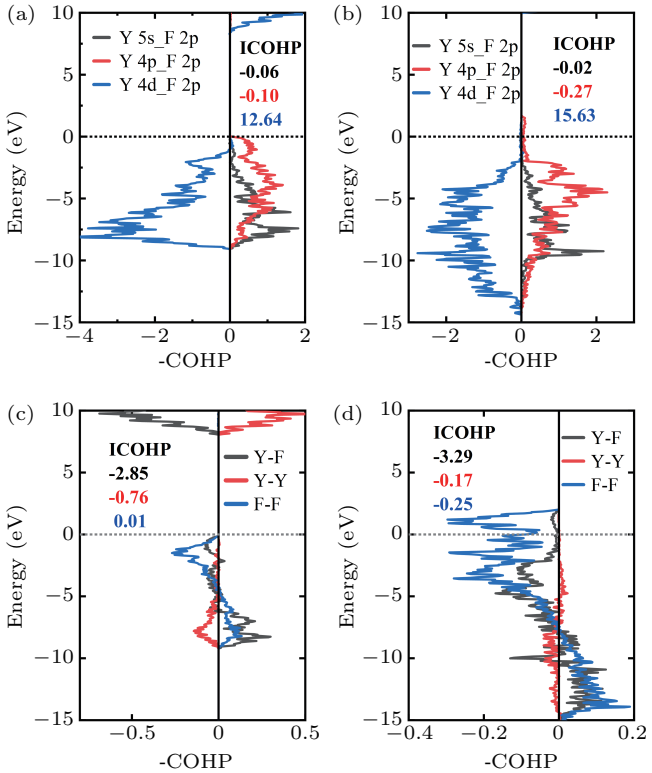


Fig. 7. COHP for (a) and (c) *Pmmn*-YF_3 at 300 GPa, and (b) and (d) *Amm*2-YF_6 at 500 GPa. The Fermi energy (black dashed line) is set to zero.

COHP calculations were performed for YF_3 and YF_6 (Fig. 7) to enhance the understanding of chemical bonding properties and formation mechanisms in Y–F compounds. COHP is employed to extract chemical bonding information regarding structural stability.[51] Bonding and antibonding interactions are associated with negative and positive COHP val-

ues, respectively, while non-bonding interactions correspond to a COHP value of zero.[51]

For *Pmmn*-YF_3 at 300 GPa, the negative COHP values between Y-5s/4p and F-2p orbitals indicate bonding interactions. A positive COHP value associated with Y-4d and F-2p orbitals indicates an antibonding interaction. The integrated crystal orbital Hamilton population (ICOHP) values for Y-5s/4p and F-2p orbital interactions are −0.06 eV and −0.10 eV, indicating their primary contribution to the stability of the Y–F bond. The large positive ICOHP value of 12.64 eV for the Y-4d and F-2p orbitals indicates a strong antibonding interaction that destabilizes the Y–F bond. Bonding interactions are indicated by negative COHP values of the Y–F and Y–Y pairs, while an antibonding interaction is associated with the positive COHP value of the F–F pair. The calculated ICOHP values reveal that bonding in YF_3 is dominated by the Y–F pairs, whereas the F–F pair shows a weak antibonding interaction with a small positive ICOHP of 0.01 eV.

For *Amm*2-YF_6 at 500 GPa, the COHP values for the Y-5s/4p orbitals and F-2p orbitals are negative, indicating bonding interactions. In contrast, the Y-4d and F-2p orbitals exhibit a positive COHP value, indicating antibonding. The ICOHP values for the Y-5s, Y-4p, and Y-4d orbitals with F-2p are −0.02 eV, −0.27 eV, and 15.63 eV, respectively. The strong antibonding interaction between Y-4d and F-2p destabilizes the Y–F bond. It is evident that the bonding character between Y and F primarily arises from the hybridization of Y-4p and F-2p orbitals, stabilizing the new structure. The Y–F, Y–Y, and F–F pairs all show negative COHP values, indicating bonding interactions. The calculated ICOHP for Y–F is −3.29 eV, confirming that the stability of the YF_6 structure mainly stems from the Y–F interaction. A key difference from YF_3 is the presence of a weak F–F bonding interaction in YF_6.

4. Conclusion

In summary, we have conducted a systematic investigation of the stable structures and electronic properties of the Y–F binary system using first-principles methods. Two new stable structures, *Pmmn*-YF_3 and *Amm*2-YF_6, were discovered. The space group of YF_3 under ambient pressure is *Pnma*, which transitions to the *Pmmn* phase at 50 GPa, remaining stable in the range of 50–500 GPa. A new compound with a stoichiometry of YF_6 was discovered, stable above 429 GPa. AIMD simulations show that all atoms in YF_3 and YF_6 vibrate around their equilibrium positions. Electronic property calculations provide insights into bonding characteristics. The Y–F bonds in YF_3 and YF_6 are primarily ionic, arising mainly from the interaction between Y-4p and F-2p orbitals. F–F bond lengths and Bader charge analysis indicate a +3 oxidation state for yttrium in *Pmmn*-YF_3. The calculated Bader charge on Y in *Amm*2-YF_6 at 500 GPa is 2.20 electrons, identical to that in *Pmmn*-YF_3 at 300 GPa, further confirming that yttrium retains the +3 oxidation state in YF_6. This research deepens the understanding of the electronic and physicochemical properties of transition metal fluorides.

Acknowledgments

This project was supported by the National Natural Science Foundation of China (Grant No. 12204280), the Natural Science Foundation of Shandong Province (Grant No. ZR2023QA131), the China Postdoctoral Science Foundation (Grant Nos. 2023T160396 and 2021M691980), and the Youth Innovation Team Plan of Colleges and Universities in Shandong Province (Grant No. 2023KJ350).

References

[1] Li P F, Mei T T, Lu Z W, Xiang L, Zhang X, Du X D, Wang J J and Chen H H 2019 *Comput. Mater. Sci.* **159** 428
[2] Samudrala G K, Tsoi G M and Vohra Y K 2012 *J. Phys.: Condens. Matter* **24** 362201
[3] Vohra Y, Olijnik H, Grosshans W and Holzapfel W 1981 *Phys. Rev. Lett.* **47** 1065
[4] Yang Q P, Lin J Y, Li F, Zhang J, Zurek E and Yang G C 2021 *Phys. Rev. Mater.* **5** 044802
[5] Lätsch L, Lam E and Copéret C 2020 *Chem. Sci.* **11** 6724
[6] Boeyens J C 2008 *Z. Naturforsch. B* **63** 199
[7] Wu M K, Ashburn J R, Torng C, Hor P H, Meng R L, Gao L, Huang Z J, Wang Y Q and Chu A 1987 *Phys. Rev. Lett.* **58** 908
[8] Hussein A A, Hussein A A and Hasan N A 2023 *J. Appl. Sci. Nanotechnol.* **3** 65
[9] Hirakawa M, Inadama S, Kikukawa K, Suzuki E and Nakasima H 2003 *Physica C* **392** 773
[10] Troyan I A, Semenok D V, Kvashnin A G, Sadakov A V, Sobolevskiy O A, Pudalov V M, Ivanova A G, Prakapenka V B, Greenberg E and Gavriliuk A G 2021 *Adv. Mater.* **33** 2006832
[11] Kong P P, Minkov V S, Kuzovnikov M A, Drozdov A P, Besedin S P, Mozaffari S, Balicas L, Balakirev F F, Prakapenka V B and Chariton S 2021 *Nat. Commun.* **12** 5075
[12] Wang Y Y, Wang K, Sun Y, Ma L, Wang Y C, Zou B, Liu G T, Zhou M and Wang H B 2022 *Chin. Phys. B* **31** 106201
[13] Liu H Y, Naumov I I, Hoffmann R, Ashcroft N and Hemley R J 2017 *Proc. Natl. Acad. Sci.* **114** 6990
[14] Du M Y, Li Z L, Duan D F and Cui T 2023 *Phys. Rev. B* **108** 174507
[15] Peng F, Sun Y, Pickard C J, Needs R J, Wu Q and Ma Y M 2017 *Phys. Rev. Lett.* **119** 107001
[16] Sun Y, Zhong X, Liu H Y and Ma Y M 2024 *Natl. Sci. Rev.* **11** nwad270
[17] Rajakumar G, Mao L B, Bao T, Wen W, Wang S F, Gomathi T, Gnanasundaram N, Rebezov M, Shariati M A and Chung I M 2021 *Appl. Sci.* **11** 2172
[18] Leblanc M, Maisonneuve V and Tressaud A 2015 *Chem. Rev.* **115** 1191
[19] Lage M M, Righi A, Matinaga F, Gesland J and Moreira R 2004 *J. Phys.: Condens. Matter* **16** 3207
[20] Gong C, Li Q J, Liu R, Hou Y, Wang J X, Dong X T, Liu B, Yang X, Yao Z and Tan X 2013 *Phys. Chem. Chem. Phys.* **15** 19925
[21] Zalkin A and Templeton D 1953 *J. Am. Chem. Soc.* **75** 2453
[22] Bezuidenhout D, Clarke K and Pretorius R 1987 *Thin Solid Films* **155** 17
[23] Zhang W W, Oganov A R, Goncharov A F, Zhu Q, Boulfelfel S E, Lyakhov A O, Stavrou E, Somayazulu M, Prakapenka V B and Konôpková Z 2013 *Science* **342** 1502
[24] Lin J Y, Zhang S T, Guan W, Yang G C and Ma Y M 2018 *J. Am. Chem. Soc.* **140** 9545
[25] Botana J, Wang X L, Hou C J, Yan D D, Lin H Q, Ma Y M and Miao M S 2015 *Angew. Chem. Int. Ed.* **54** 9280
[26] Wang X L, Lin H Q, Ma Y M and Miao M S 2012 arXiv:1206.2874 [cond-mat.mtrl-sci]
[27] Zhang J R, Liu H Y, Ma Y M and Chen C F 2022 *Natl. Sci. Rev.* **9** nwab168

[28] Zhang J R, Liu H Y, Chen C F and Ma Y M 2024 *Matter Radiat. Extremes* **9**
[29] Li Q Y, Han S, Zhang X H, Ding S, Bergara A and Yang G C 2025 *Supercond. Sci. Technol.* **15** 100196
[30] Wang Y C, Lv J, Zhu L and Ma Y M 2010 *Phys. Rev. B* **82** 094116
[31] Wang Y C, Lv J, Zhu L and Ma Y M 2012 *Comput. Phys. Commun.* **183** 2063
[32] Kohn W and Sham L J 1965 *Phys. Rev.* **140** A1133
[33] Perdew J P, Chevary J A, Vosko S H, Jackson K A, Pederson M R, Singh D J and Fiolhais C 1992 *Phys. Rev. B* **46** 6671
[34] Perdew J P, Burke K and Ernzerhof M 1996 *Phys. Rev. Lett.* **77** 3865
[35] Kresse G and Furthmüller J 1996 *Phys. Rev. B* **54** 11169
[36] Togo A and Tanaka I 2015 *Scr. Mater.* **108** 1
[37] Dronskowski R and Bloechl P E 1993 *J. Phys. Chem.* **97** 8617
[38] Huang P H, Liu H Y, Lv J, Li Q, Long C H, Wang Y C, Chen C F, Hemley R J and Ma Y M 2020 *Proc. Natl. Acad. Sci. USA* **117** 5638
[39] Olson M A, Bhatia S, Larson P and Militzer B 2020 *J. Chem. Phys.* **153**
[40] Tantardini C, Jalolov F N and Kvashnin A G 2022 *J. Phys. Chem. C* **126** 11358
[41] Lv Q Q, Jin X L, Cui T, Zhuang Q, Li Y, Wang Y C, Bao K and Meng X 2017 *Chin. Phys. B* **26** 076103
[42] Li Y W, Hao J, Liu H Y, Tse J S, Wang Y C and Ma Y M 2015 *Sci. Rep.* **5** 9948
[43] Savin A, Nesper R, Wengert S and Fässler T F 1997 *Angew. Chem. Int. Ed.* **36** 1808
[44] Adachi G-y and Imanaka N 1998 *Chem. Rev.* **98** 1479
[45] Wang F X, Rui Q, Jiang Q W, Li J F, Zhu H Y, Wang Q L and Wang X L 2022 *Solid State Commun.* **358** 115001
[46] Sievers M, Chen Y M and Armentrout P 1996 *J. Chem. Phys.* **105** 6322
[47] Barnes L A, Rosi M and Bauschlicher Jr C W 1990 *J. Chem. Phys.* **93** 609
[48] Lin J Y, Du X, Rahm M, Yu H, Xu H Y and Yang G C 2020 *Angew. Chem. Int. Ed.* **59** 9155
[49] Lin J Y, Zhao Z Y, Liu C Y, Zhang J, Du X, Yang G C and Ma Y M 2019 *J. Am. Chem. Soc.* **141** 5409
[50] Checkelsky J G, Bernevig B A, Coleman P, Si Q M and Paschen S 2024 *Nat. Rev. Mater.* **9** 509
[51] Steinberg S and Dronskowski R 2018 *Crystals* **8** 225